

Understanding Cold Denaturation: The Case Study of Yfh1

Miquel Adrover,^{†,‡} Veronica Esposito,[†] Gabriel Martorell,[§] Annalisa Pastore,^{*,†} and Piero Andrea Temussi^{*,†,||}

MRC National Institute for Medical Research, The Ridgeway, London NW7 1AA, United Kingdom, Department de Química, Universitat de les Illes Balears, Palma de Mallorca, E07122, Spain, Serveis Científic-Tècnics, Universitat de les Illes Balears, Palma de Mallorca, E07122, Spain, and Department of Chemistry, Università di Napoli Federico II, via Cinthia, 80126 Napoli, Italy

Received August 17, 2010; E-mail: apastor@nimr.mrc.ac.uk; temussi@unina.it

Abstract: All globular proteins undergo transitions from their native to unfolded states if exposed either to cold or to heat perturbation. While the heat-induced transition is well described for a large number of proteins, in media compatible with natural environments, the limited number of examples of cold denatured states concern proteins artificially destabilized, for instance, by the presence of denaturants, ad hoc point mutations, or both. Here, we provide a characterization of the low temperature unfolded state of Yfh1, a natural protein that undergoes cold denaturation around water freezing temperature, in the absence of any denaturant. By achieving nearly full assignment of the NMR spectrum, we show that at -1 °C, Yfh1 has all the features of an unfolded protein, although retaining some local, residual secondary structure. The effect is not uniform along the sequence and does not merely reflect the secondary structural features of the folded species. The N-terminus seems to be dynamically more flexible, although retaining some nascent helix character. Interestingly, this region is the one containing functionally important hot-spots. The β -sheet region and the C-terminal helix are completely unfolded, although experiencing some conformational exchange, partly due to the presence of several prolines. Ours is the first step toward a full characterization of the low temperature unfolded state of a natural protein, reached without the aid of any destabilizing agent. We discuss the implications of our findings for understanding cold denatured states.

Introduction

Understanding the forces that govern protein folding and stability constitutes a major challenge, which has involved and still involves generations of biophysicists. It is well-known that the temperature range in which proteins retain their native fold can vary significantly for different proteins and is determined by the complex balance of mutually competing stabilizing and destabilizing forces. However, while many decades of biophysical studies have led to the identification of the main forces that lead to protein unfolding caused by thermal denaturation, many phenomena that are connected with the action of intramolecular forces at low temperature remain poorly understood.

Yet, it is now widely recognized that proteins also undergo “cold denaturation”, which is a transition from the folded to unfolded state, at temperatures below room temperature.¹ It is a property of globular proteins well predicted by the Gibbs–Helmholtz equation and believed to be driven by the hydration of polar and nonpolar groups as well as the decrease of hydrophobic interactions.² Cold denaturation has been well characterized thermodynamically by various techniques such as CD and calorimetry.¹ However, to date, still little is known at a detailed structural level of cold denatured proteins. The main

reason why cold denaturation has not been explored more thoroughly is that this process is difficult to study because, for most proteins, it occurs at temperatures well below freezing of aqueous solutions. To circumvent this difficulty, several researchers have tried either to design ways to keep water in a supercooled condition or to raise the temperature of cold denaturation, mainly by destabilizing the protein through mutations and/or addition of denaturants.^{3–5} The obvious drawback of approaches based on artificial denaturation of proteins is the difficulty of extrapolating the results to physiological conditions.

Recently, we have serendipitously identified a protein, Yfh1, whose cold denaturation occurs at temperatures above 0 °C and at physiological conditions.⁶ Yfh1 is the yeast orthologue of frataxin, a mitochondrial human protein responsible for the neurodegenerative disease Friedreich’s ataxia.⁷ The frataxin family is highly conserved both in sequence and in structure from bacteria to humans and is essential for life. Despite their conservation, the thermodynamic stability of different orthologues varies appreciably.⁸ Of the three best characterized orthologues, Yfh1 is the protein with the lowest and the highest

[†] MRC National Institute for Medical Research.

[‡] Department de Química, Universitat de les Illes Balears.

[§] Serveis Científic-Tècnics, Universitat de les Illes Balears.

^{||} Università di Napoli Federico II.

(1) Privalov, P. L. *Crit. Rev. Biochem. Mol. Biol.* **1990**, *25*, 281–305.

(2) Privalov, P. L.; Gill, S. J. *Adv. Protein Chem.* **1988**, *39*, 191–234.

(3) Chen, B.; Schellman, J. *Biochemistry* **1989**, *232*, 600–679.

(4) Wong, K.-B.; Freund, S. M. V.; Fersht, A. R. *J. Mol. Biol.* **1996**, *259*, 805–818.

(5) Shan, B.; McClendon, S.; Rospigliosi, C.; Eliezer, D.; Raleigh, D. *J. Am. Chem. Soc.* **2010**, *132*, 4669–4677.

(6) Pastore, A.; Martin, S. R.; Politou, A.; Kondapalli, K. C.; Stemmler, T.; Temussi, P. A. *J. Am. Chem. Soc.* **2007**, *129*, 5374–5375.

(7) Pandolfo, M.; Pastore, A. *J. Neurol.* **2009**, *256*, 9–17.

thermal stabilities at high and low temperatures, respectively, having the two melting points around 5 and 35 °C when in its apo form.⁶ These features, together with the fact that Yfh1 is a protein from natural sources rather than an “ad hoc” designed mutant, make it a system uniquely suited for an extensive characterization of the cold transition and of the factors influencing its stability as a function of temperature. For instance, using this system, we have been able to show that alcohols, rightly considered as denaturing agents at high concentrations, behave as stabilizers of native protein folds at low concentration and low temperature.⁹

Here, we present a structural characterization of the cold denatured state of Yfh1 using NMR studies in solution, a technique that allows a detailed study of protein fold also when it is in a highly dynamical state. We have assigned the spectrum of Yfh1 at −1 °C, a task per se quite demanding. From our results, we show that at this temperature the protein is unfolded, although there are indications that it retains local, residual secondary structure in regions that map around functionally important hotspots. This is to our knowledge the first example of such an analysis for a naturally occurring protein without the need of solvent and/or fold perturbation.

Experimental Section

Sample Preparation. Recombinant *S. cerevisiae* Yfh1 was produced as previously described in detail.^{10,11} In short, the protein was expressed in *Escherichia coli* BL21-(DE3) cells grown at 37 °C, induced in 1 mM IPTG for 6 h, lysed with a French press, and sonicated. The soluble, overexpressed protein was purified by two ammonium sulfate precipitation steps with a 40% cut to precipitate contaminating proteins and a 65% cut to precipitate Yfh1. After dialysis, the protein was subjected to anion exchange chromatography using a Pharmacia Q-Sepharose column with a gradient to 1 M NaCl, followed by a Pharmacia phenyl-Sepharose column with a decreasing 1 M ammonium sulfate gradient. An EDTA-containing protease inhibitor cocktail tablet (Roche) was added before the cells were lysed and at each purification step. EDTA and salts were removed by dialysis prior to concentration of the protein. ¹⁵N-labeled and ¹⁵N,¹³C double-labeled samples were produced by growing the bacteria in minimal medium using ammonium sulfate and glucose as the sole source of nitrogen and carbon.

NMR Spectroscopy. ¹⁵N- and ¹⁵N,¹³C-labeled Yfh1 samples used for NMR studies (~0.5 mM) were dialyzed to 20 mM Hepes at pH 7.0 and 2 mM DTT, containing 10% (v/v) D₂O. Multidimensional NMR experiments were carried out at −1 °C on a Varian Nova spectrometer operating at 14.1 T and equipped with an inverse triple-resonance single-axis gradient probe. ¹H, ¹⁵N HSQC,¹² ¹⁵N-TOCSY-HSQC¹³ (70 ms mixing time), ¹⁵N NOESY-HSQC¹⁴ (200 ms mixing time), HNCA,¹⁵ HN(CO)CA,¹⁵ HNCACB,¹⁶ and CACB(CO)HN¹⁷ experiments were performed to enable sequence-

specific backbone assignment and to assign the protons and the ¹³C_β of the side chains. Each residue was assigned only after observing a perfect match between all the described backbone experiments. Water was suppressed by the Watergate pulse sequence.¹⁸ Proton chemical shifts were referenced to the water signal fixed at 5.0 ppm. ¹³C and ¹⁵N chemical shifts were referenced indirectly using the ¹H, X frequency ratios of the zero-point.¹⁹ All spectra were processed using NMRpipe/NMRDraw²⁰ and analyzed by Easy/CARA²¹ and Sparky²² software. A Gaussian window function was applied to process the ¹H dimensions of the 2D HSQC and the 3D NOESY experiments.

Chemical shift indices (CSI)²³ and secondary structure propensity (SSP) scores²⁴ were calculated using the <http://www.bionmr.ualberta.ca/bds/software/csi/latest/csi.html> and the <http://pound.med.utoronto.ca/software.html> servers, respectively. Helix propensity was estimated using the AGADIR program.²⁵

The assigned chemical shifts of Yfh1 at −1 °C are deposited in BioMagResBank (<http://www.bmrb.wisc.edu>) under accession number 17068.

Results

Cold Denaturation of Yfh1 Is Highly Cooperative. We have previously demonstrated that Yfh1 undergoes unbiased cold denaturation at temperatures around 0 °C.⁶ Because the exact temperature of cold denaturation can slightly vary as a function of ionic strength, we were very careful in excluding even minute quantities of spurious salts in the preparation of the NMR sample.

¹⁵N HSQC spectra are considered one of the fingerprints of a given protein. The ¹⁵N HSQC spectrum of Yfh1 at −1 °C has all the features typical of an unfolded protein, with overall poor resonance dispersion, especially in the ¹H dimension (Figure 1A). The degree of unfolding could be estimated analyzing symptomatic peaks: the resonances of the side chain indole groups of the two tryptophans (W80 and W98), which are well distinct in the folded state, collapse into a unique resonance at 10.2 and 129.5 ppm in the HSQC spectrum of the low temperature denatured state.

The intensity of the high field resonances at −0.65 and −0.45 ppm, present in the 1D proton spectrum of folded Yfh1, also decreases abruptly around the transition temperature,⁶ leading to a complete absence of the resonances at −1 °C (Figure 1B). These high field peaks typically originate from aliphatic residues in persistent spatial proximity of aromatic groups, which provide an additional local magnetic field and are highly diagnostic for correct folded proteins.

Taken together, these results suggest that the cold denaturation process is highly cooperative and leads to a mostly unstructured state.

NMR Spectral Assignment Suggests Different Dynamical Properties along the Yfh1 Sequence. Peak picking of the resonances observed in the ¹⁵N HSQC spectrum led to a total

- (8) Adinolfi, S.; Nair, M.; Politou, A.; Bayer, E.; Martin, S.; Temussi, P.; Pastore, A. *Biochemistry* **2004**, *43*, 6511–6518.
- (9) Martin, S. R.; Esposito, V.; De Los Rios, P.; Pastore, A.; Temussi, P. A. *J. Am. Chem. Soc.* **2008**, *130*, 9963–9970.
- (10) Adinolfi, S.; Trifuoggi, M.; Politou, A.; Martin, S.; Pastore, A. *Hum. Mol. Genet.* **2002**, *11*, 1865–1877.
- (11) He, Y.; Alam, S. L.; Proteasa, S. V.; Zhang, Y.; Lesuisse, E.; Dancis, A.; Stemmler, T. L. *Biochemistry* **2004**, *43*, 16254–16262.
- (12) Bodenhausen, G.; Ruben, D. L. *Chem. Phys. Lett.* **1980**, *69*, 185–188.
- (13) Palmer, A. G.; Cavanagh, J.; Wright, P. E.; Rance, M. *J. Magn. Reson.* **1991**, *93*, 151–170.
- (14) Davis, A. L.; Keeler, J.; Laue, E. D.; Moskau, D. *J. Magn. Reson.* **1992**, *98*, 207–216.
- (15) Grzesiek, S.; Bax, A. *J. Magn. Reson.* **1992**, *96*, 432–440.
- (16) Wittekind, M.; Mueller, L. *J. Magn. Reson., Ser. B* **1993**, *101*, 201–205.
- (17) Grzesiek, S.; Bax, A. *J. Biomol. NMR* **1993**, *3*, 185–204.

- (18) Piotto, M.; Saudek, V.; Sklenár, V. *J. Biomol. NMR* **1992**, *2*, 661–665.
- (19) Wishart, D. S.; Bigam, C. G.; Yao, J.; Abildgaard, F.; Dyson, H. J.; Oldfield, E.; Markely, J. L.; Sykes, B. D. *J. Biomol. NMR* **1995**, *2*, 135–140.
- (20) Delaglio, F.; Grzesiek, S.; Vuister, G. W.; Zhu, G.; Pfeifer, J.; Bax, A. *J. Biomol. NMR* **1995**, *6*, 277–293.
- (21) Bartels, C.; Xia, T. H.; Billeter, M.; Güntert, P.; Wüthrich, K. *J. Biomol. NMR* **1995**, *6*, 1–10.
- (22) Goddard, T. D.; Kneller, D. G. *SPARKY 3*; University of California: San Francisco, 2008.
- (23) Wishart, D. S.; Sykes, B. D.; Richards, F. M. *Biochemistry* **1992**, *31*, 1647–1651.
- (24) Marsh, J. A.; Singh, V. K.; Jia, Z.; Forman-Kay, J. D. *Protein Sci.* **2006**, *15*, 2795–2804.
- (25) Muñoz, V.; Serrano, L. *Nat. Struct. Biol.* **1994**, *1*, 399–409.

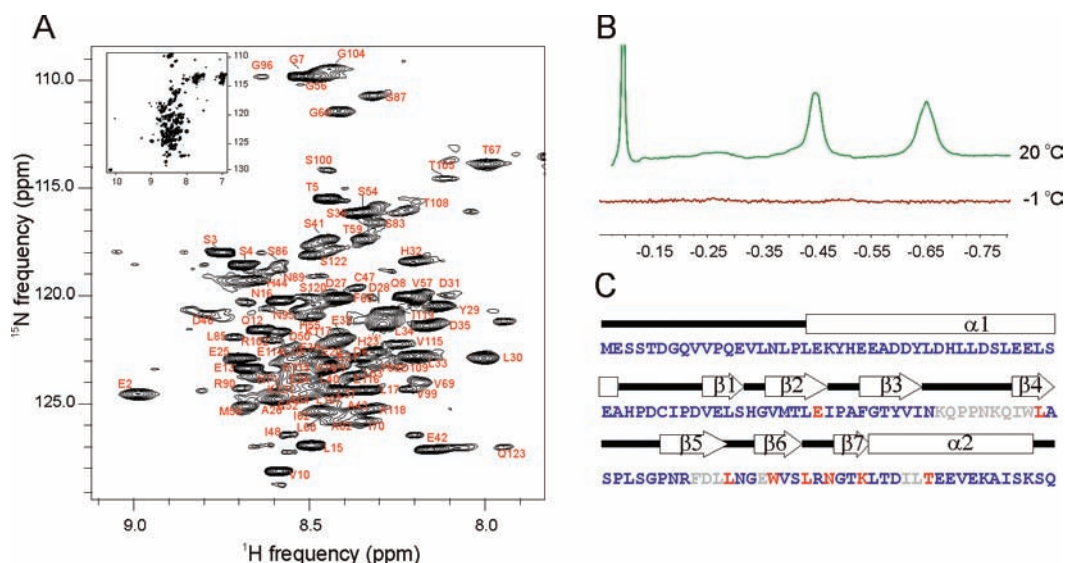


Figure 1. Characterization of the cold denatured state of Yfh1 from its NMR spectrum. (A) Close-up of high-resolution ^{15}N HSQC spectrum of Yfh1 in 20 mM Hepes at pH 7.0 at -1°C and 600 MHz, labeled with assignments. Inset: The whole ^{15}N HSQC spectrum. The spectrum was collected using 256 increments in the nitrogen dimension and a 2K spectral width in the direct dimension. (B) Comparison of the high-field regions of the Yfh1 spectra recorded at -1 and 20°C and 600 MHz. (C) Sequence of Yfh1 annotated for the secondary structure elements.¹¹ Helices and strands are indicated with ribbons and arrows, respectively. Assigned residues are indicated in blue, residues for which only partial assignment could be done are in red, and unidentified residues are shown in gray.

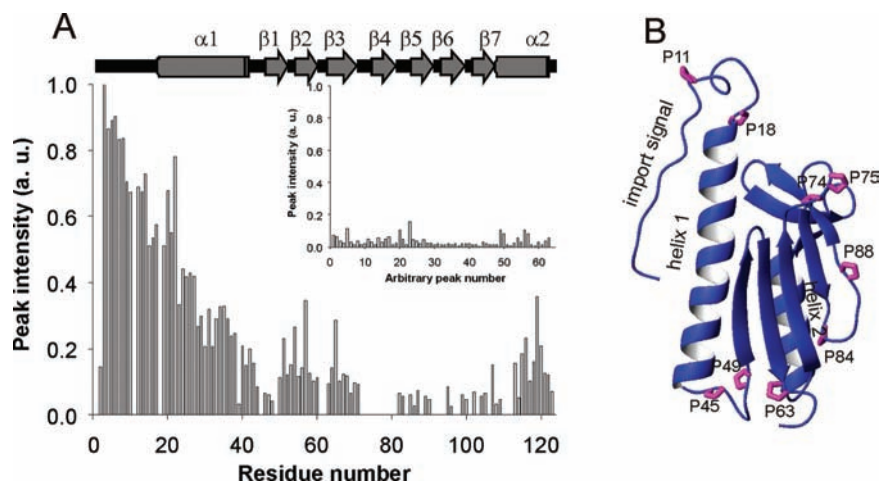


Figure 2. Plot of the resonance intensities, as estimated from the high-resolution ^{15}N HSQC spectrum and mapping the effects onto the native structure. (A) Parent plot: The intensities of the assigned peaks are plotted as a function of the protein sequence. The secondary structure is indicated on the plot for reference. Inset: The intensities of the extra unassigned resonances are plotted using arbitrary peak numbers. (B) Ribbon representation of the tertiary structure of Yfh1 (PDB code 2ga5) at 25°C . The fold contains an N-terminal import signal (residues 1–12) followed by two helices (helix 1 and helix 2), which sandwich a six-strands β -sheet. The side chains of proline residues are indicated.

of 190 peaks that is appreciably more than the total number of expected resonances (i.e., 138 when considering 114 nonproline residues, 2 tryptophan indoles, and 11 H_2N side chain groups) (Figure 1A). The peak intensities are, however, greatly variable with intense sharp peaks in copresence with weak resonances.

Unambiguous sequential assignment (^1H , ^{15}N , ^{13}C) could be achieved, despite the severe resonance overlap, for 81% of the residues (Figure 1C) by using the ^{15}N NOESY-HSQC and triple resonance experiments to trace the backbone assignment (Figure S1, Supporting Information). A relatively small set of residues (M1, E61, K72-L81, F91-L94, E97, W98, L101, N103, K106, I110, L111, and T112) remained partially or completely unassigned because their resonances could not be traced in the spectrum. These residues are mostly clustered in the β -sheet, suggesting that these structural elements are affected by some conformational exchange. When peak intensities were plotted

as a function of the sequence, it became evident that the sharper and more intense peaks belong to N-terminal residues (Figure 2A). They correspond to the signal peptide, which imports Yfh1 into mitochondria and which is likely to be unfolded and flexible also in the native structure, and helix 1.⁷ In addition to peaks from the main species, almost completely assigned, 60 additional unassigned peaks could be identified in the ^{15}N HSQC. The intensities of all the additional resonances are, however, comparably weaker (Figure 2A, inset). These observations provide independent evidence of a different dynamical behavior of different regions of Yfh1 in the cold denatured state.

Cis/Trans Proline Isomerization in the Cold Denatured State. Assignment allowed us to clarify the role of at least some of the additional resonances. While some of them might well be noise, others are clearly double species having the same spin system and the same connectivities of already assigned residues.

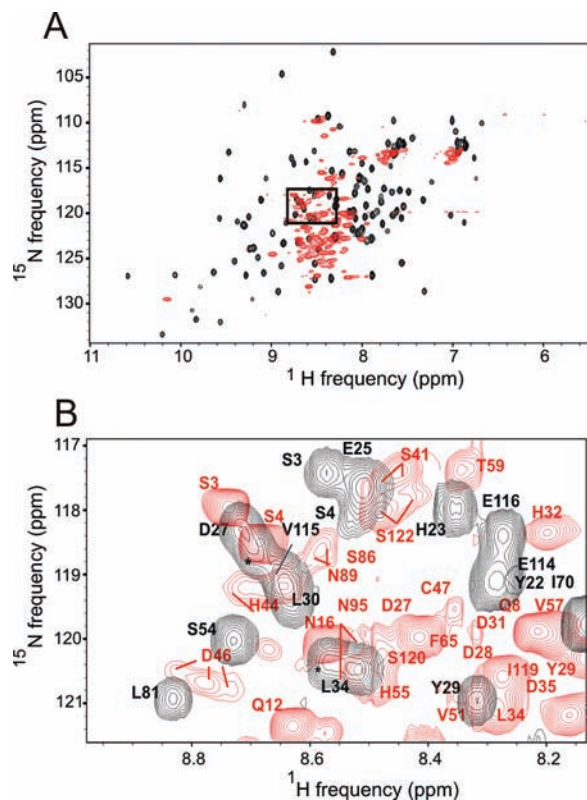


Figure 3. Evidence for multiple conformations. (A) Superposition of the ^{15}N HSQC spectra of Yfh1 recorded at $-1\text{ }^{\circ}\text{C}$ (red peaks) and at $25\text{ }^{\circ}\text{C}$ (black peaks). Both spectra were recorded using 20 mM Hepes solution at pH 7.0 at 600 MHz. (B) Close-up of a small portion of the spectrum in (A) showing the double peaks observed for several resonances, for example, N95, and triple peaks observed for D46. The assignments at $25\text{ }^{\circ}\text{C}$ are those of He et al.¹¹ The peaks indicated with asterisks are unassigned peaks. Extra peaks do not correspond to resonances observed in the native spectrum.

Their chemical shifts are well distinct from those of the same residue in the native species, thus ruling out the possibility that they could arise from the copresence of folded and unfolded species in slow equilibrium (Figure 3A). We could, for instance, clearly detect double resonances for residues like V10, L19, S41, D46, D50, S54, A64, A82, N95, V115, E116, S120, and S122. Interestingly, five of these residues directly precede or follow a proline, suggesting that the duplicate species arise from cis/trans isomerization (Figure 3B). In support of this view is the observation that at least three species are present for D46, a residue that is sandwiched between two prolines (Figure 1C). Because no isomerization has been reported for the native state,¹¹ the effect is likely to become detectable only in the unfolded state.

Analysis of the $\text{C}\alpha$ and $\text{C}\beta$ chemical shifts of the prolines at $-1\text{ }^{\circ}\text{C}$ suggests that in the main species they all represent trans conformations, with the only possible exception for P84, which has an upfield shifted $\text{C}\alpha$ (62.1 ppm) and a low-field shifted $\text{C}\beta$ (32.6 ppm) as compared to literature values (i.e., 61.9 and 30.6 ppm for a trans proline and 61.4 and 33.0 ppm for a cis proline).²⁶

Indications of a Solvation Effect at Low Temperature. To discriminate among sequential, structural, and/or solvation effects on the chemical shifts, the ^{15}N and ^{13}C HSQC spectra at $-1\text{ }^{\circ}\text{C}$ were compared to the corresponding simulated spectra,

obtained by plotting random coil values at room temperature,²⁷ corrected for next neighbors effects²⁸ (Figure 4).

Simulated and experimental spectra present interesting similarities and differences. In $\text{H}\alpha$ – $\text{C}\alpha$ spectra (panel A), the differences between the simulated spectrum (right panel) and the experimental one at $-1\text{ }^{\circ}\text{C}$ (left panel) are small. Overall, the same residue type remains in both spectra in roughly corresponding regions of the spectrum, although the actual distribution may be different. The small spread of the resonances in the experimental spectrum apparently suggests that the low temperature state does not have marked conformational preferences.

On the contrary, differences between corresponding clusters of the same residue are rather pronounced for the proton–nitrogen correlation spectra (Figure 4B). Outstanding examples are the Glu, Gln, and Ser residues, whose values differ up to 1.0 and 10 ppm in the proton and nitrogen frequencies, respectively. In addition, it is possible to notice that there is also an overall downshift tendency, both for ^1H and for ^{15}N values. It is tempting to attribute this effect to a much more efficacious hydration at low temperature. This comparison strongly suggests that the marked differences between experimental and random coil values must reflect not only sequential effects but also specific features of the conformational ensemble at low temperature.

Residual Secondary Chemical Shifts Indicate Residual Helical Propensity. The secondary chemical shifts, that is, the difference between the tabulated²⁷ random coil values at $25\text{ }^{\circ}\text{C}$ and the observed ones, were analyzed for $\text{H}\alpha$, $\text{C}\alpha$, and $\text{C}\beta$ atoms, because these groups have a higher sensitivity to the secondary structure. Plots of $\text{H}\alpha$ chemical shifts for the regions 1–20 and 40–123 show that they are shifted upfield by a maximum of ~ 0.1 ppm, whereas in the region 21–39 the $\Delta\delta$ values are ~ 0.23 ppm upfield. Consistently, $\text{C}\alpha$ chemical shifts of the regions 19–42 and 97–123 are shifted ~ 0.5 ppm downfield as compared to the random coil values, whereas the $\text{C}\alpha$ chemical shifts for the majority of the other residues are randomly shifted upfield and downfield by ~ 0.2 ppm. To make sure that what we observe is independent from referencing, the $\Delta\delta\text{C}\alpha$ – $\Delta\delta\text{C}\beta$ differences were also considered (see Figure S2, Supporting Information). In all three plots, the main outliers are V10, L17, H44, I48, I62, S83, and G87. Interestingly, these residues all precede a proline.

To reveal possible indications of residual secondary structure in the cold denatured state, we analyzed the chemical shift indexes along the sequence.²³ The indices of the $\text{H}\alpha$ protons could suggest some helical propensity in correspondence of helix 1 (Figure 5A). However, the consensus values over $\text{H}\alpha$, $\text{C}\alpha$, and $\text{C}\beta$ atoms indicate no secondary structure propensity along the whole sequence.

Because chemical shift indices could be a rather insensitive method, as they involve a yes-or-not answer, we used two additional approaches. We first calculated the smoothed secondary shifts of $\text{H}\alpha$ protons according to the method suggested by Pastore and Saudek.²⁹ Smoothing is sufficient to average out the noise introduced by local environmental factors, providing a sensitive and specific way to detect secondary structure elements. This method suggests some helical propensity in the region 20–40, near the C-terminus and in correspondence with

(27) Wishart, D. S.; Bigam, C. G.; Holm, A.; Hodges, R. S.; Sykes, B. D. *J. Biomol. NMR* **1995**, *5*, 67–81.

(28) Wang, Y.; Jardetzky, O. *J. Am. Chem. Soc.* **2002**, *124*, 14075–14084.

(29) Pastore, A.; Saudek, V. *J. Magn. Reson.* **1990**, *90*, 165–176.

(26) Richarz, R.; Wüthrich, K. *Biopolymers* **1978**, *17*, 2263–2269.

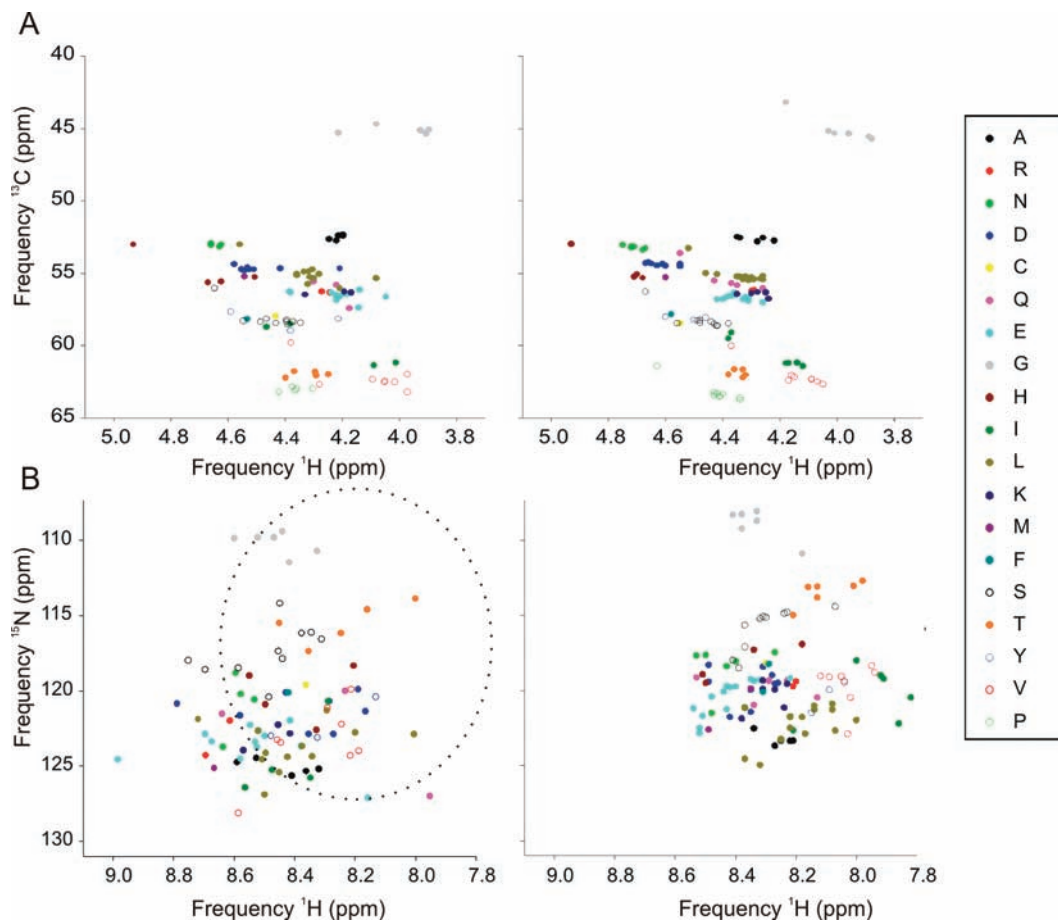


Figure 4. Estimate of the next neighboring effect in HSQC spectra of cold denatured Yfh1. (A) Comparison of a simulated ^{13}C HSQC spectrum (right) with the experimental spectrum (left). Random coil shifts are corrected for the nature of the previous and following residue.²⁸ Different residues are indicated in different colors as shown in the legend on the right. (B) Comparison of a simulated ^{15}N HSQC spectrum (right) with the experimental spectrum (left). Random coil shifts are corrected for the nature of the previous and following residue.²⁸ The dotted line oval in the left spectrum corresponds to the total area span by all peaks in the simulated spectrum. Different residues are indicated in different colors as shown in the legend on the right.

some of the loops between the β -strands (Figure 5B). Similar results were obtained using the SSP indices,²⁴ which show residual helical propensity mainly in correspondence with helix 1 (Figure 5C). Interestingly, the region 20–40 comprises helix 1, which seems to have a lower helical propensity than helix 2 as estimated by the AGADIR program²⁵ at $-1\text{ }^\circ\text{C}$ (Figure 5D).

NOE Effects at Low Temperature. The quality of the ^{15}N -NOESY-HSQC at low temperature is excellent despite spectral overlap. Practically all residues are visible and have NOESY effects, although mostly local and/or sequential (Figure 6A). Several observations can be made on the basis of this spectrum. Virtually in all strips, the sequential $\text{H}\alpha_i\text{--HN}_{i+1}$ are more intense than the intraresidual connectivity, indicating extended structures. No $\text{H}\alpha$ resonances have chemical shifts below 5 ppm, which are typical of β -sheet conformations, thus suggesting absence of this secondary structure, in agreement with the secondary chemical shift analysis. If we assume instead the presence of $\text{HN}_i\text{--HN}_{i+1}$ effects as diagnostic for residual, albeit local, secondary structure (e.g., turns or nascent helix), the residues can be classified into three distinct classes (Figure 6B): (a) residues that do not have sequential HN--HN ; (b) residues that have sequential HN--HN connectivities as they do also at $25\text{ }^\circ\text{C}$; and (c) residues that do not adopt helical or helical like structures at $25\text{ }^\circ\text{C}$ but have an HN--HN connectivity at $-1\text{ }^\circ\text{C}$. The first class comprises the large majority of the residues all along the sequence, regardless of the structure they have in

the folded species. The second class comprises most but not all residues of helix 1 and practically almost no residues of helix 2, suggesting that the former has a stronger nascent helix character than the latter. This is interestingly at variance with what is expected from calculations of helical propensity by the AGADIR program,²⁵ which gives for helix 2 a much higher propensity than for helix 1 at all temperatures. The third class comprises ca. 16 residues.

Among them, the most interesting are the N-terminal residues in the signal peptide, and up to seven additional residues, which are in the β -sheet in the folded species. These residues indicate some tendency to adopt non-native like structures at low temperature.

Discussion

We have presented here a detailed NMR analysis of the properties of the cold denatured state of Yfh1, a small yeast protein whose human orthologue is associated with undergoing cold and heat denaturation at temperatures closer to room temperature than those of most proteins. There is sparse information about proteins at low temperature mostly because these conditions are outside the physiologic range for most proteins. This is especially true for NMR studies, considering that low temperatures increase spectral line broadening and disfavor through-bond connectivities. As illustrated by Figure S3 (Supporting Information), which reports the distribution of

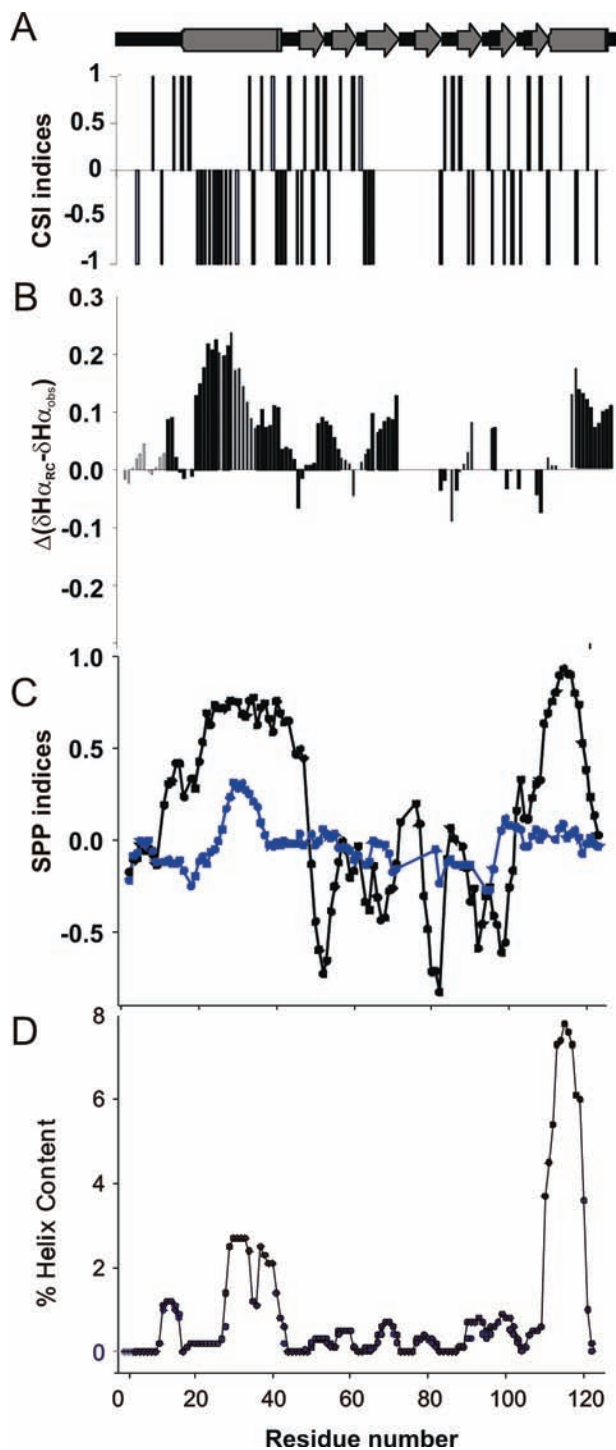


Figure 5. Secondary structure indicators at $-1\text{ }^{\circ}\text{C}$ and helical propensity plotted versus the Yfh1 sequence. (A) CSI indices of the $\text{H}\alpha$ protons.²⁵ (B) Smoothed plot of the secondary chemical shifts of the $\text{H}\alpha$ protons.²⁷ (C) SPP values of Yfh1, as calculated from HN, N, $\text{H}\alpha$, $\text{C}\alpha$, and $\text{C}\beta$ chemical shift values at pH 7.0 and $-1\text{ }^{\circ}\text{C}$ (blue line) and $25\text{ }^{\circ}\text{C}$ (black, values from He et al.¹¹).²⁴ (D) Helical propensity at $-1\text{ }^{\circ}\text{C}$ as estimated by the AGADIR software.²⁵ The secondary structure of the native protein is indicated on the top for reference.

proteins whose NMR spectral assignment is available in the BRBM database, there are very few examples of proteins characterized at low temperature by NMR, particularly at temperatures close to $0\text{ }^{\circ}\text{C}$. The few examples available are mainly intrinsically unfolded proteins or proteins from psychrophilic organisms. To our knowledge, Yfh1 is therefore the

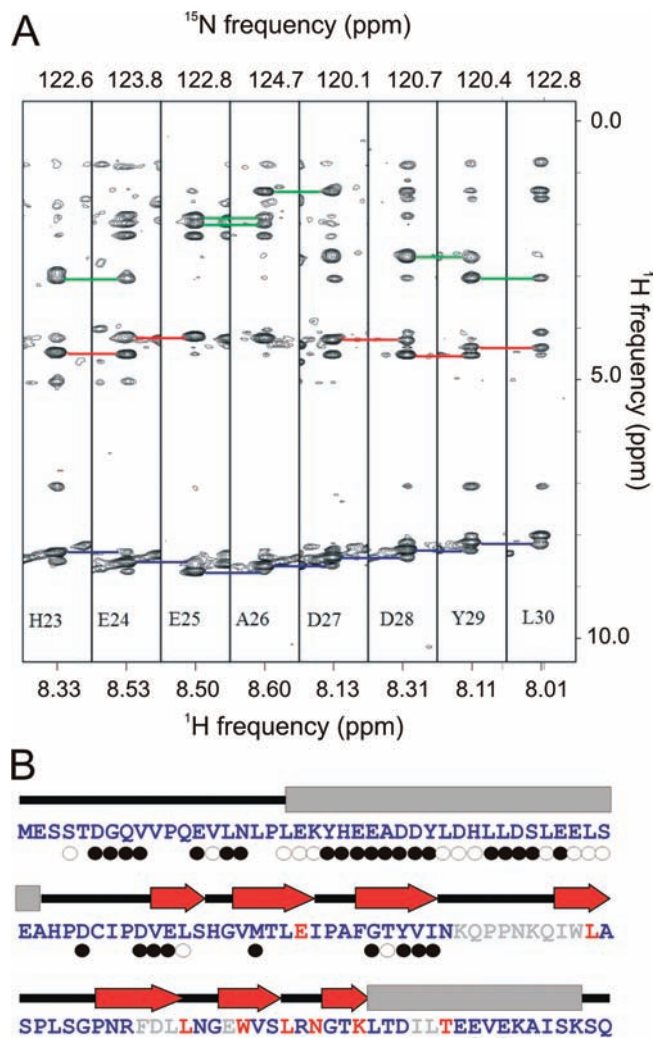


Figure 6. Indications of residual secondary structure from NOE effects. (A) Representative strips of a 3D ^{15}N NOESY-HSQC spectrum of Yfh1 at $-1\text{ }^{\circ}\text{C}$ and 600 MHz. Blue lines mark HN–HN, red lines indicate HA–HN, and green lines indicate HB–HN NOEs, respectively. (B) $\text{HN}_i\text{HN}_{i+1}$ effects observed along the sequence and their correlation with the secondary structure observed at $25\text{ }^{\circ}\text{C}$. The “●” on residue i indicate the presence of an $\text{HN}_i\text{HN}_{i+1}$ connectivity. The “○” indicate residues for which the diagonal peaks have the same chemical shifts, making the presence of a connectivity impossible to exclude.

first example of a full-length natural protein that can undergo cold denaturation at temperatures accessible to NMR analysis, without the need of addition of destabilizing cosolvents and/or introduction of ad hoc mutations. We thus exploited these properties to characterize the cold denatured state and addressed the question of whether and, in case, how much does the cold denatured state retain the features typical of the folded one. A virtually full assignment of the NMR spectrum of Yfh1 at $-1\text{ }^{\circ}\text{C}$ allowed us to draw a number of conclusions.

An important result of our work is that we do not observe any marked similarity between the cold denatured state and the native one, as proven by the difference in chemical shifts, which do not support any possible copresence of the native and denatured state.

This poor similarity is at variance with a recent study of I98A–CTL9, a destabilizing point mutant of the C-terminal domain of the ribosomal protein CTL9.⁵ In this study, the authors suggest that the low temperature unfolded state has many

of the conformational features typical of the folded one. While this could be in principle due to different dynamical properties of the Yfh1 and CTL9 proteins, it is useful to bear in mind that the NMR assignment of the unfolded state of CTL9 was performed at a temperature close to the mid point of the cold transition, that is, a state that, by definition, should contain ca. 50% of folded protein in equilibrium with the unfolded form. In addition, I98A–CTL9, although being an interesting model system, like many older literature cases is not a native protein, leaving the doubt that the results of its study could not allow straightforward extrapolation to a generic native protein. Similar considerations apply also to another case of full NMR assignment of a cold denatured protein, that of a double mutant of Barstar.⁴ The authors used the full assignment (¹H, ¹⁵N, ¹³C) of this protein in 3 M urea at 5 °C to assess residual structure, using a variety of secondary structure indicators. They also found a good correspondence with the structure of the folded species, particularly in the regions corresponding to the first and the second helices and near the end of the second β -strand of native barstar. However, it is difficult to compare their results with ours because, as previously pointed out, we did not add denaturants to our solutions.

We have also shown that at low temperature Yfh1 has chemical shifts similar to but in many ways also distinctly different from the random coil values tabulated at 25 °C. The difference does not simply reflect nearest neighbor effects and must be explained by other causes such as solvation effects, which are consistent with the overall downfield shift as compared to the expected unfolded spectrum. This observation is particularly relevant for the cold denatured state because, according to the currently accepted mechanism of cold denaturation,¹ hydration plays a key role in this process. Privalov¹ has shown that cold denaturation is caused by the temperature-dependent interaction of nonpolar groups of the protein with water. Counterintuitively, hydration of protein nonpolar groups is thermodynamically favorable and increases in magnitude at a temperature decrease. As a result, the polypeptide chain unfolds at a sufficiently low temperature, exposing internal nonpolar groups to water. Our direct observation of the strong hydration of most amide groups in the cold denatured state of Yfh1 is fully consistent with this model.

Additionally, secondary chemical shifts and NOE effects strongly suggest the presence of specific regions with nascent helix character.³⁰ They comprise both regions adopting helical (helix 1) but also β -structures in the folded protein. These observations are consistent with the concept of chameleon sequences:³¹ it is now commonly accepted knowledge that the same protein sequence can adopt different secondary structures when in isolation or in the context of the full-length protein, in which the tertiary contacts may modulate or even invert the secondary structure tendency of a given sequence.

We observe, in the unfolded state of Yfh1, a clearly different dynamical behavior along the sequence. The N-terminus, approximately up to the end of what forms helix 1 in the folded state, seems to be the most flexible part, suggesting a more cooperative collapse of this region upon unfolding. Resonances

from the C-terminus, some of which can hardly be identified, are overall less intense and possibly undergo conformational exchange.

These results suggest an interesting caveat concerning the relationship between flexibility and structure: it seems unwise to draw conclusions about the conformational preferences of a sequence on the basis of apparent flexibility alone. At first sight, the data of Figure 2 might imply that the N-terminal residues are very flexible and therefore less structured than other parts of the sequence, as one would automatically assume in the case of several intrinsically unfolded proteins. However, the analysis of all other secondary structure indicators shows convincingly that the very same region retains more secondary structure than the remaining regions of the sequence. The low intensity of the resonances from the central part of the sequence can be attributed to conformational exchange among several unstructured species, dominated by cis–trans proline isomerism. Thus, it seems fair to conclude that, although helix 1 is the first secondary structure element to collapse, it is also the most persistent one in retaining a secondary structure in the cold denatured species.

Finally, it is very interesting to note that the only significant element of residual secondary structure present in the cold denatured species, the nascent helix corresponding in part to helix 1 of the folded species, contains highly conserved residues that play a key role in the function of frataxins. It is now widely accepted that frataxins bind iron and other divalent and trivalent cations through conserved residues all clustered on helix 1. The same region was recently demonstrated to be also involved in interaction with IscS, the desulfurase enzyme central to iron–sulfur cluster formation.³² It is thus tempting to suggest that persistence of a nascent helix character can be also important both for the stability of the frataxin/IscS complex and for iron binding.

In conclusion, our data provide new insights into the early events that cause protein folding and give us a glimpse into the effects that low temperature forces have onto protein structure. The next important step will be to deepen the dynamical analysis of the unfolded state of Yfh1 by recording additional NMR parameters and by comparing the cold and heat denatured states for the same protein to assess how these two unfolded states compare with each other.

Acknowledgment. We are indebted to Geoff Kelly of the MRC NMR Centre for technical support. A.P. and P.A.T. also thank the Faculty of the Chemistry Department and Serveis Científic-Tecnic of the University of Balearic Islands for warm hospitality. We wish to thank Thomas Szyperski (Buffalo, NY) and Eldon Ulrich (BRMB, Madison, WI) for the nice graph of Figure S3 in the Supporting Information. We gladly acknowledge financial support from the University of Balearic Islands and from an International JOINT PROJECT of the Royal Society (NIMR: U.1175.03.002.00001.04).

Supporting Information Available: HNCACB spectrum of Yfh1; unsmoothed secondary chemical shifts of Yfh1; and distribution of numbers of protein structures determined by NMR as a function of temperature. This material is available free of charge via the Internet at <http://pubs.acs.org>.

JA1070174

(30) Dyson, H. J.; Rance, M.; Houghten, R. A.; Wright, P. E.; Lerner, R. A. *J. Mol. Biol.* **1988**, *201*, 201–217.

(31) Ghozlane, A.; Joseph, A. P.; Bornot, A.; de Brevern, A. *Bioinformation* **2009**, *4*, 367–369.

(32) Adinolfi, S.; Iannuzzi, C.; Prischi, F.; Pastore, C.; Iametti, S.; Martin, S. R.; Bonomi, F.; Pastore, A. *Nat. Struct. Mol. Biol.* **2009**, *16*, 390–306.